

SI Appendix
for
Histone deacetylases control module-specific
phenotypic plasticity in beetle weapons

Takane Ozawa^a, Tomoko Mizuhara^a, Masataka Arata^b, Masakazu Shimada^c,
Teruyuki Niimi^d, Kensuke Okada^e, Yasukazu Okada^{c,1}, Kunihiro Ohta^{a,b,1}

^aDepartment of Life Sciences, Graduate School of Arts and Sciences, The University of Tokyo, Meguro, Tokyo 153-8902, Japan

^bDepartment of Biological Sciences, Graduate School of Science, The University of Tokyo, Bunkyo, Tokyo 113-0033, Japan

^cDepartment of General Systems Studies, Graduate School of Arts and Sciences, The University of Tokyo, Meguro, Tokyo 153-8902, Japan

^dDivision of Evolutionary Developmental Biology, National Institute for Basic Biology, 38, Nishigonaka, Myodaiji, Okazaki 444-8585, Japan

^eLaboratory of Evolutionary Ecology, Graduate School of Environmental Science, Okayama University, Okayama, Okayama 700-8530, Japan

¹Corresponding authors: Yasukazu Okada (Meguro, Tokyo 153-8902, Japan, +81-3-5454-6974, okayasukazu@gmail.com) and Kunihiro Ohta (Meguro, Tokyo 153-8902, Japan, +81-3-5454-8834, kohta@bio.c.u-tokyo.ac.jp)

SI Materials and Methods

Insect husbandry

Our stock population of *G. cornutus* originated from adults collected in Miyazaki City (31°54', 131°25'), Japan, and maintained at the National Food Research Institute and Okayama University (1). *G. cornutus* was reared as described previously (2). In brief, larvae of *G. cornutus* were reared in groups in plastic containers (65 mm in diameter and 45 mm in height) supplied with whole meal flour enriched with yeast. The larvae were developmentally arrested at the final-instar stage under crowding conditions of stock culture, and they became prepupae 3 to 4 days after isolation (2). We obtained final-instar larvae destined to become prepupae by isolating them in wells of a 24-well tissue culture plate (Thermo scientific). We defined the larvae of 1-2 mg body weight as penultimate instar larvae. The larvae were subjected to drug administrations or gene knockdowns. Rearing and experiments were performed in a chamber maintained at 25°C, 60% relative humidity, and a photoperiod cycle of 16-/8-h light/dark conditions.

Double-stranded RNA synthesis

Total RNA was extracted from the prepupal whole body of *G. cornutus* by using the SV Total RNA Isolation System (Promega). First-strand cDNA was synthesized using the SuperScriptII FS kit (Invitrogen) with 1 µg of total RNA. Double-stranded RNA (dsRNA) was synthesized using the Ambion MEGAscript® T7 Transcription Kit (Invitrogen). DNA template for in vitro transcription was produced with PCR by using gene-specific primers with the T7 polymerase promoter at their 5' ends (Table S5). DNA template of GFP was produced using primers GFPiF2 and GFPiR5 (3). PCR products were purified and concentrated using the Wizard® SV Gel and PCR Clean-Up System (Promega) and subjected to in vitro transcription and dsRNA purification, according to the manufacturer's protocol. The reaction mix was purified and concentrated by phenol-chloroform extraction and sodium acetate/ethanol precipitation. dsRNA was quantified and diluted to 1 µg/µl and stored at -80°C.

Microinjection of epigenetic drugs and dsRNA

Final-instar larvae were randomly selected from the stock culture. Stock solutions of trichostatin A (TSA, 2 $\mu\text{g}/\mu\text{l}$ dimethyl sulfoxide: DMSO), an inhibitor of class I histone deacetylases, and 5-azacytidine (5-AzaC, 10 $\mu\text{g}/\mu\text{l}$ water), an inhibitor of DNA methyltransferases, were prepared. Dosage was optimized to produce maximal non-lethal effects by the stated criteria (TSA: 46 ng/larva, 5AzaC: 3.48 $\mu\text{g}/\text{larva}$) and drugs were injected into the dorsal side of the abdominal segment of the larvae by using NANOJECT II (DRUMMOND) under CO₂ anesthesia. The injected final instar larvae were individually isolated in 24-well culture plates (Thermo scientific), so that they could develop into prepupae (the adult morphogenetic stage) within 3 to 4 days (2, 4). No food was provided after the treatment. The developmental stage of the injected larvae was observed once a day. Individuals that successfully became adults were used for measurements.

dsRNA was also injected in the final-instar and penultimate instar larvae. Injected penultimate instar larvae were reared for 3 weeks under crowding condition until they became final-instar larvae, and they were individually isolated in 24-well culture plates (Thermo scientific). Stock solutions of dsRNA (1 $\mu\text{g}/\mu\text{l}$ water) for each target gene were prepared. To avoid any systemic developmental failures due to high doses of RNAi, dsRNA dose adjustment was performed as described in Table S5. In HDAC1 and HDAC3 knockdowns at penultimate instar larvae, a dsRNA dose for “early KD” in Table S5 was used for experiments of gene-knockdown efficiencies (Fig. S3 D and E) and morphological measurements (Fig. 2 G and H, and Fig. S5). In the morphological observations and measurements of adults subjected to HDAC1, HDAC3 RNAi, moderate doses were used to avoid severe defects during pupal maturation and adult eclosion.

Morphological observations and measurements

Morphological observations of pupae and adults were performed using a scanning electron microscope (SEM; VE-8800, KEYENCE). To evaluate the morphogenetic effects of epigenetic perturbations, 16 body parts of adult males were quantified (Fig.

1B) using mandible sizes (length, outline length, and width) as indices of exaggerated traits. Elytra width was considered as an index of body size and used as a covariate to examine the effect of the treatments on trait sizes (5, 6).

Straight-line distances between two landmark points were measured with the microscope monitoring system (VHX-200, KEYENCE), and curvature structures (mandible outline length, wing vein lengths, and genitalia length; Fig. 1B) were measured as curve-fitted lengths by using the segmental line tool in Image J (7) with captured digital images. Adult males were randomly selected from each treatment for the measurements. The measurements were performed on right sides of appendages. In case of accidental damage to the wings and legs, left sides were used for the analysis. All analyses were performed using R 3.1.1 (8) and JMP 11.

Sequencing of Genes for HDACs and PcGs in *G. cornutus*

Transcript sequences of the *G. cornutus* orthologs for HDACs, PcG genes, DNA methylation factors and histone modification factors were identified using *de novo* RNA-seq. Total RNA was isolated from the heads of final-instar larvae and prepupae (24 and 48 h after attaining the prepupal stage) by using the Ambion RNAqueous®-Micro Total RNA Isolation kit (Invitrogen). RNA quality was tested using Agilent Bioanalyzer 2100. cDNA was synthesized using the template-switching method (9). cDNA library samples were run using an Illumina HiSeq 2000 platform for 100 cycles with paired-end reads at the Beijing Genomics Institute. Quality of the sequencing reads was assessed with the software FastQC (<http://www.bioinformatics.babraham.ac.uk/projects/fastqc/>), and the reads were quality-filtered (Q20) and trimmed (3 nt from 3' end) with the FastX-toolkit software suite (http://hannonlab.cshl.edu/fastx_toolkit/). The adaptor sequence of every read was eliminated using Tagdust (10). The quality-filtering paired-end read results showed that some reads lost their partner reads. All post-processed reads were pooled together and assembled *de novo* with Trinity (11, 12) (Trinity version: Trinityrnaseq_r20131110). We obtained 412,824 contigs by *de novo* assembly with Trinity. *G. cornutus* orthologs of histone-modifying genes were identified using the

KEGG Automatic Annotation Server (KAAS) (13) with manual checks of sequence similarities to *T. castaneum* orthologs. The DNA Data Bank of Japan (DDBJ)/European Molecular Biology Laboratory (EMBL)/GenBank accession numbers for Gc-HDACs and Gc-PcGs are listed in Table S4.

In addition, cross-species gene orthologies (*G. cornutus*, *T. castaneum*, *D. melanogaster*, and *H. sapiens*) were confirmed by phylogenetic relationships of proteins by using MEGA 6.0 (14) with a heuristic search under JTT models with 1000 bootstrap replicates.

Quantitative RT-PCR for HDAC expression analysis

cDNA was prepared from the head, thorax, abdomen and whole body of dsRNA injected larvae and prepupae. Quantitative RT-PCR was performed using the KAPA SYBR Fast qPCR Kit (KAPA BIOSYSTEMS) with Applied Biosystems® StepOnePlus™. Actin gene Gc-ACT was used as the reference for comparative Ct quantification. Primer sequences for the actin gene, HDACs, and PcG genes are listed in Table S10.

SI References

1. Okada K & Miyatake T (2010) Effect of losing on male fights of broad-horned flour beetle, *Gnatocerus cornutus*. *Behav Ecol Sociobiol* 64(3):361-369.
2. Ozawa T, Ohta K, Shimada M, Okada K, & Okada Y (2015) Environmental Factors Affecting Pupation Decision in the Horned Flour Beetle *Gnatocerus cornutus*. *Zool Sci* 32(2):183-187.
3. Tomoyasu Y & Denell R (2004) Larval RNAi in *Tribolium* (Coleoptera) for analyzing adult development. *Dev Genes Evol* 214(11):575-578.
4. Okada Y, Gotoh H, Miura T, Miyatake T, & Okada K (2012) Juvenile hormone mediates developmental integration between exaggerated traits and supportive traits in the horned flour beetle *Gnatocerus cornutus*. *Evol Dev* 14(4):363-371.
5. Okada K & Miyatake T (2009) Genetic correlations between weapons, body shape and fighting behaviour in the horned beetle *Gnatocerus cornutus*. *Anim Behav* 77(5):1057-1065.
6. Okada K & Miyatake T (2010) Plasticity of size and allometry in multiple sexually selected traits in an armed beetle *Gnatocerus cornutus*. *Evol Ecol* 24(6):1339-1351.
7. Schneider CA, Rasband WS, & Eliceiri KW (2012) NIH Image to ImageJ: 25 years of image analysis. *Nat Meth* 9(7):671-675.
8. Team RC (2012) A language and environment for statistical computing [computer program]. *Vienna, Austria: Foundation for Statistical Computing*.
9. Aird SD, *et al.* (2013) Quantitative high-throughput profiling of snake venom gland transcriptomes and proteomes (*Ovophis okinavensis* and *Protobothrops flavoviridis*). *BMC genomics* 14(1):790.
10. Lassmann T, Hayashizaki Y, & Daub CO (2009) TagDust—a program to eliminate artifacts from next generation sequencing data. *Bioinformatics* 25(21):2839-2840.
11. Grabherr MG, *et al.* (2011) Trinity: reconstructing a full-length transcriptome without a genome from RNA-Seq data. *Nat Biotechnol* 29(7):644-652.
12. Haas BJ, *et al.* (2013) De novo transcript sequence reconstruction from RNA-Seq: reference generation and analysis with Trinity. *Nat Protoc* 8(8):10.1038/nprot.2013.1084.
13. Moriya Y, Itoh M, Okuda S, Yoshizawa AC, & Kanehisa M (2007) KAAS: an automatic genome annotation and pathway reconstruction server. *Nucleic Acids Res* 35(suppl 2):W182-W185.
14. Tamura K, Stecher G, Peterson D, Filipowski A, & Kumar S (2013) MEGA6: molecular evolutionary genetics analysis version 6.0. *Mol Biol Evol* 30(12):2725-2729.

SI Figures

Figure S1

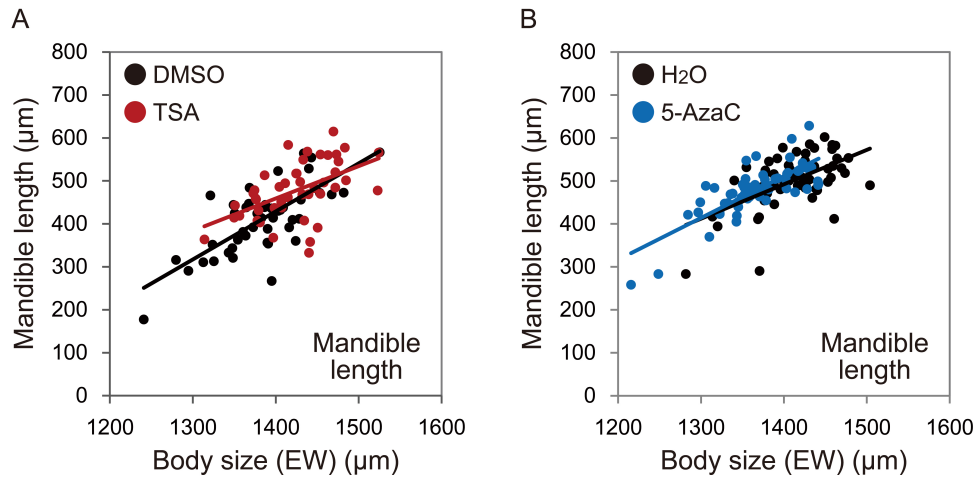


Fig. S1. Effects of epigenetic inhibitor treatments on mandible size in *G. cornutus* males. (A) The effects of TSA treatment on mandible size. DMSO (control, black dots and lines) and TSA treatment (red dots and lines) are shown. (B) The effect of 5-azacytidine (AzaC) treatment on mandible size. H₂O (control, black dots and lines) and 5-AzaC treatment (blue dots and lines) are shown. ANCOVA results are summarized in Table S2.

Figure S2

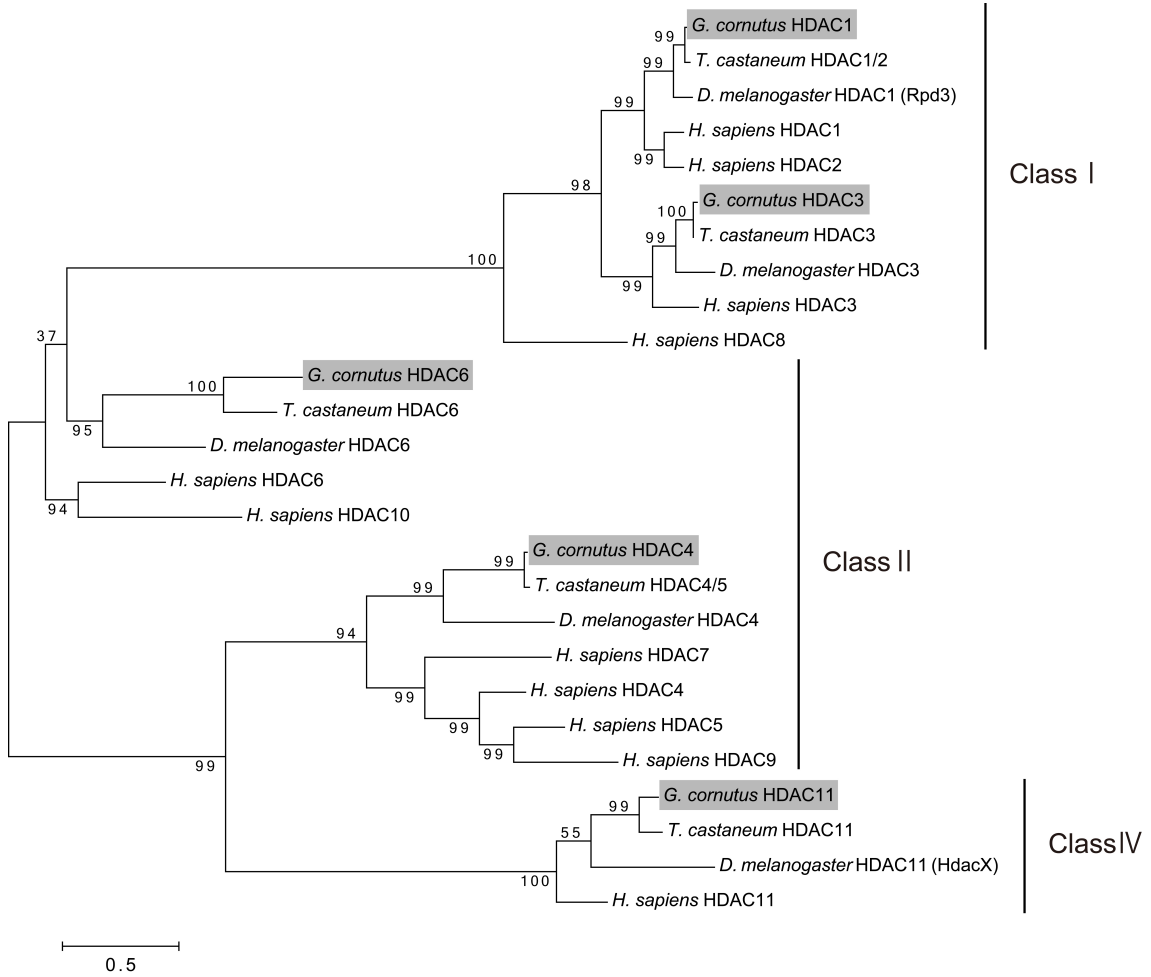


Fig. S2. Orthological relationships of HDACs in *G. cornutus* and other model species. Phylogeny is based on amino acid sequences. *G. cornutus* HDACs are highlighted in gray. Numbers on branches indicate maximum likelihood bootstrap values (1,000 replicates).

Figure S3

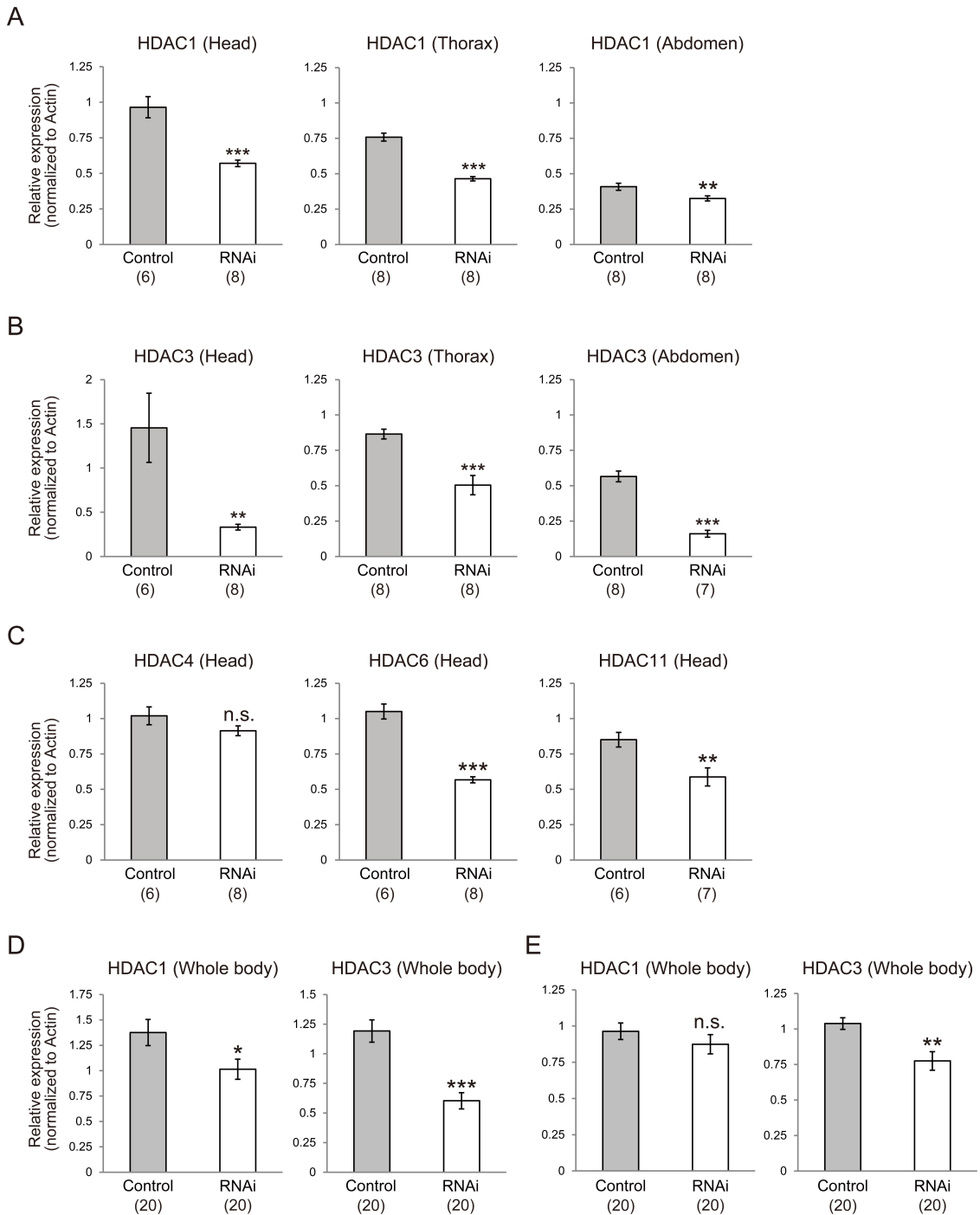


Fig. S3. Gene-knockdown efficiencies of HDAC RNAi. (A-C) Relative transcript abundances for HDAC1 (A), HDAC3 (B), HDAC4, HDAC6, and HDAC11 (C) in prepupae after gene-knockdowns at final-instar larvae. Left to right columns in A and B show transcript levels in head, prothorax, or abdomen. (D, E) Relative transcript abundances for HDAC1 and HDAC3 in penultimate instar larvae (D) and

prepupae (E) after gene-knockdowns at penultimate instar larvae. Left and right columns in D and E show transcript levels in whole body. Mean \pm SE values are shown (*, $P < 0.05$; **, $P < 0.01$; ***, $P < 0.001$; n.s., not significant, t -test). Numbers within parentheses indicate sample sizes.

Figure S4

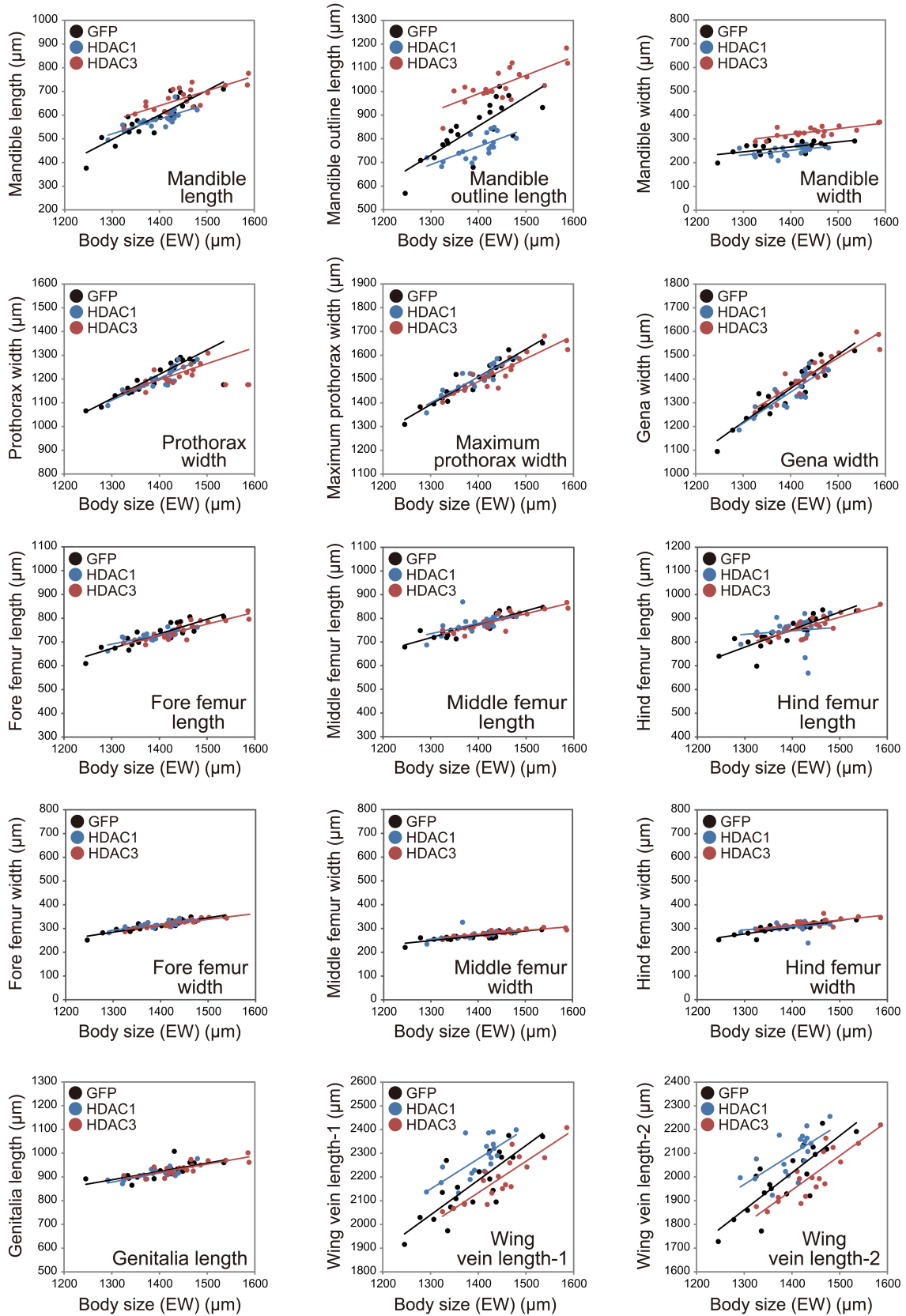


Fig. S4. Effects of HDAC1 and HDAC3 late-knockdowns on trait sizes in *G. cornutus* males. GFP knockdown (control, black dots and lines), HDAC1 knockdown (blue dots and lines), and HDAC3 (red dots and lines) are shown. ANCOVA results are summarized in Table S6.

Figure S5

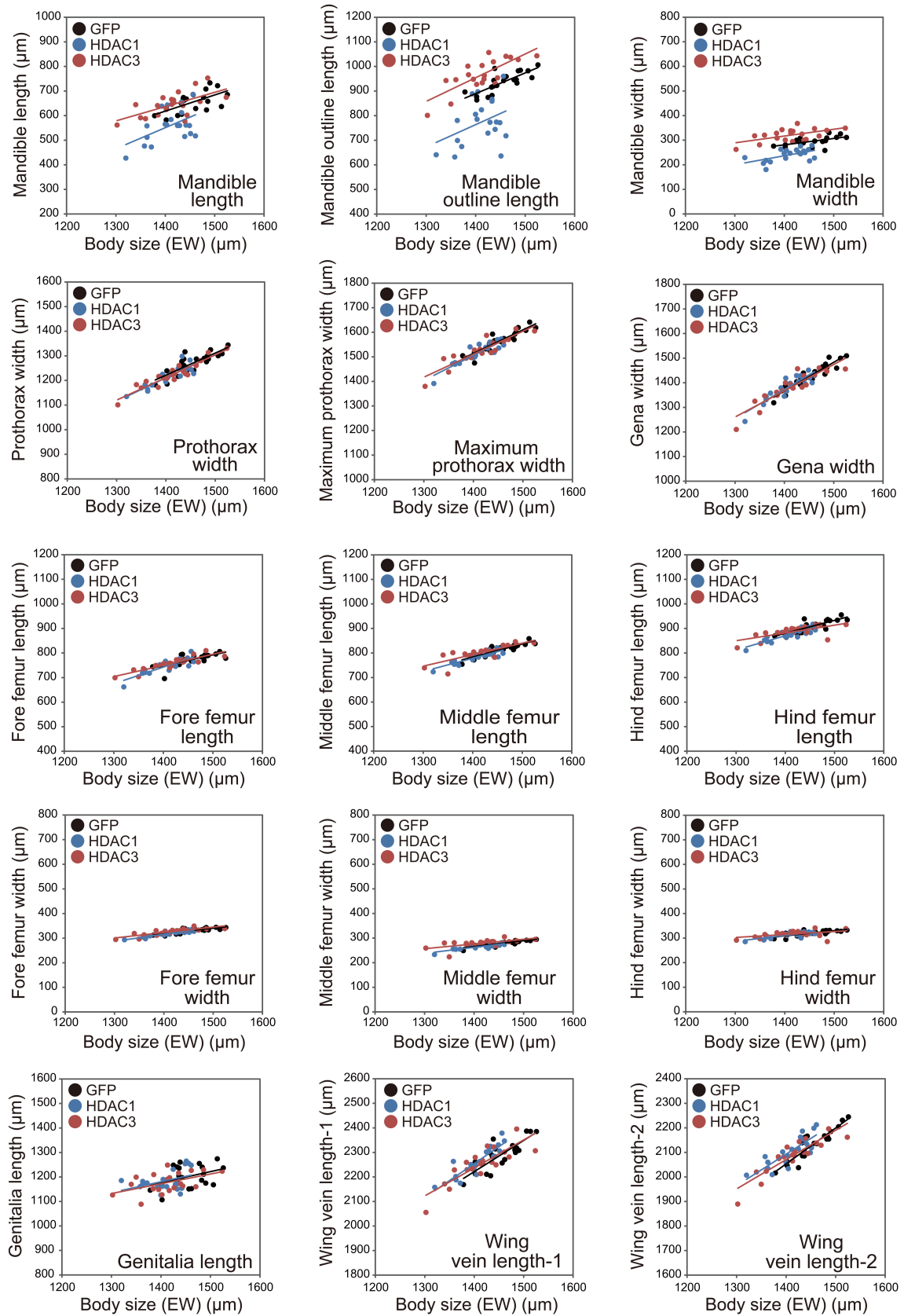


Fig. S5. Effects of HDAC1 and HDAC3 early-knockdowns on trait sizes in *G. cornutus* males. GFP knockdown (control, black dots and lines), HDAC1 knockdown (blue dots and lines), and HDAC3 (red dots and lines) are shown. ANCOVA results are summarized in Table S7.

Figure S6

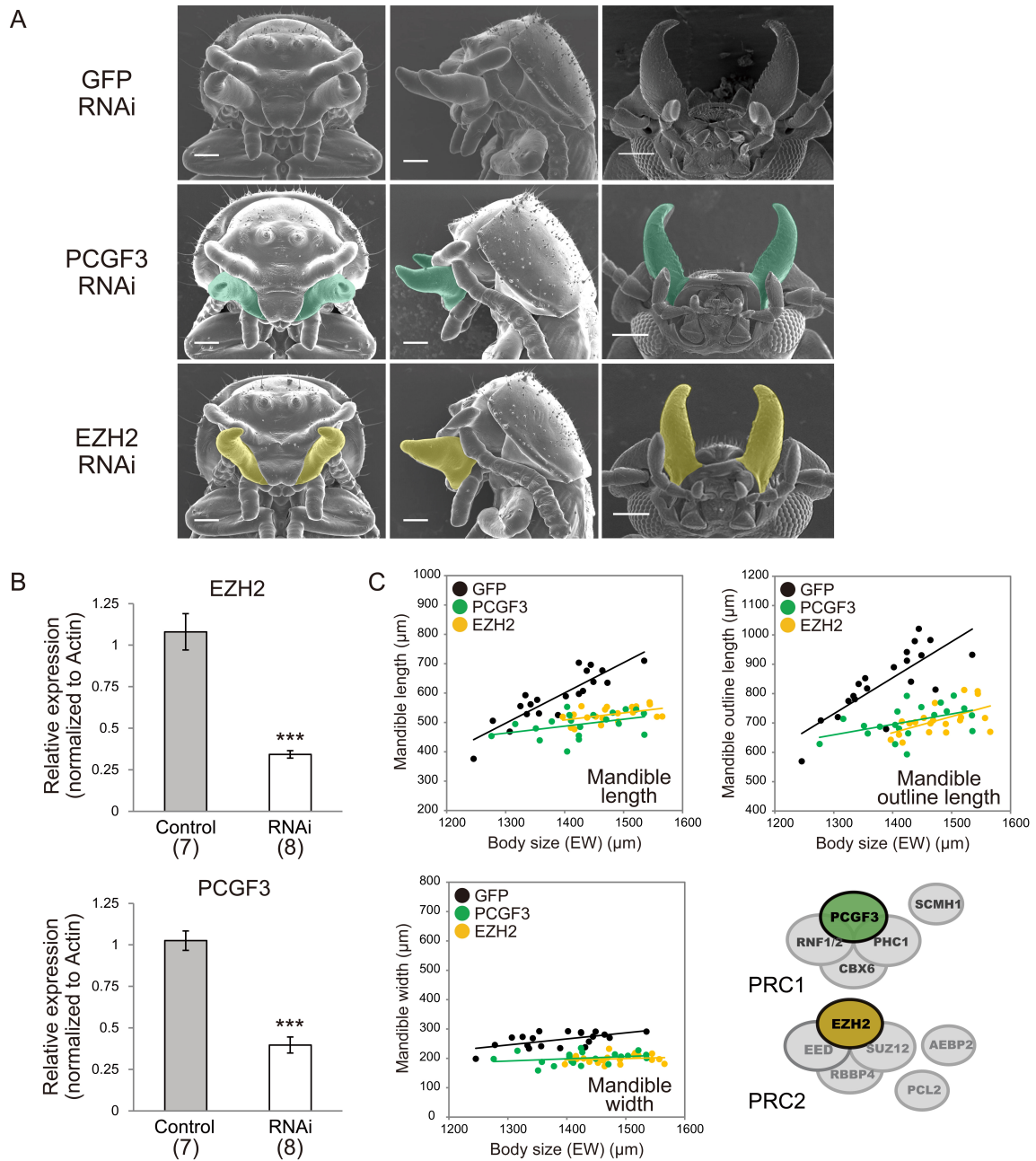


Fig. S6. Effects of knockdowns of polycomb group (PcG) proteins on pupal and adult morphologies. (A) EZH2 and PCGF3 knockdowns reduce pupal and adult mandible sizes. Male heads of pupae (front and side views, left and middle columns) and adults (ventral view, right column) for GFP, EZH2, or PCGF3 RNAi are shown. Mandibles are indicated in green (PCGF3) or yellow (EZH2). Scale bars indicate 200 μm. (B) Gene knockdown efficiencies of EZH2 or PCGF3 in the heads of prepupae.

Mean \pm SEM values are shown. (***, $P < 0.001$, t -test). Numbers within parentheses indicate sample size. (C) PCGF3 and EZH2 knockdowns that significantly reduce mandible sizes in *G. cornutus* males (GFP control, black dots and line; PCGF3 knockdown, green dots and line; and EZH2 knockdown, yellow dots and line) are shown. Statistical results are shown in Table S9.

SI Tables

Table S1. Variability in exaggerated and somatic/genital traits of male *Gnatocerus cornutus*.

Trait	Allometric coefficient (95% confidence interval)	
mandible length (ML)	2.58	(1.87 - 3.28)
mandible outline length (MOL)	2.16	(1.33 - 2.98)
mandible width (MW)	1.16	(0.38 - 1.94)
gena width (GW)	1.49	(1.22 - 1.76)
prothorax width (PW)	1.18	(1.05 - 1.31)
maximum prothorax width (MPW)	1.08	(0.93 - 1.24)
fore femur length (FFL)	1.19	(0.88 - 1.51)
fore femur width (FFW)	1.38	(1.08 - 1.69)
middle femur length (MFL)	1.02	(0.76 - 1.28)
middle femur width (MFW)	1.07	(0.70 - 1.43)
hind femur length (HFL)	1.22	(0.83 - 1.61)
hind femur width (HFW)	1.34	(0.97 - 1.72)
genitalia length (GL)	0.53	(0.24 - 0.81)
wing vein length-1 (WVL-1)	0.94	(0.61 - 1.28)
wing vein length-2 (WVL-2)	1.1	(0.74 - 1.45)

Bold letters in allometric coefficients show statistically significant values ($\alpha > 1$ [positive allometry] or $\alpha < 1$ [negative allometry] at 95% confidence intervals).

Table S2. Effects of TSA and 5-azacytidine (AzaC) treatments on mandible sizes.

Trait	Relative size change (% of control)	Sample size		Effect (treatment)		Effect (treatment x elytra width)	
		Control	Treatment	<i>F</i>	<i>P</i>	<i>F</i>	<i>P</i>
TSA treatment							
mandible length (ML)	6.30%	46	45	4.421	0.038	2.221	0.140
5-AzaC treatment							
mandible length (ML)	3.60%	60	56	3.339	0.070	0.826	0.365

Relative trait means were calculated as estimated marginal means (adjusted means) at mean body size with elytra width as a covariate by ANCOVA. Bold letters indicate significant size changes when compared with the control treatment.

Table S3. Summary of the read statistics from RNA sequencing and *de novo* transcriptome assembly.

total reads	
Total number of reads	446,191,805
Total nucleotides (nt)	45,065,372,305
High-quality reads	430,939,602
Total length of high quality reads (bp)	43,524,899,802
Assembly	
Total assemble nucleotides (nt)	932,155,473
Total number of transcripts	412,824
Median transcript length (bp)	1,507
Average transcript length (bp)	2,258
N50 size (bp)	4,025
GC content (%)	41.14

Table S4. Candidate epigenetic genes in *G. cornutus*.

<i>G. cornutus</i> gene	Description of KEGG	KO	Accession No.
HDACs (histone deacetylases)			
Class I HDACs			
HDAC1	HDAC1_2; histone deacetylase 1/2 [EC:3.5.1.98]	K06067	LC096257
HDAC3	HDAC3; histone deacetylase 3 [EC:3.5.1.98]	K11404	LC096258
Class II HDACs			
HDAC4	HDAC4_5; histone deacetylase 4/5 [EC:3.5.1.98]	K11406	LC096259
HDAC6	HDAC6; histone deacetylase 6 [EC:3.5.1.98]	K11407	LC096260
Class IV HDACs			
HDAC11	HDAC11; histone deacetylase 11 [EC:3.5.1.98]	K11418	LC096261
Polycomb group proteins			
PRC1 (polycomb repressive complex 1)			
CBX6 *	CBX8, PC3; chromobox protein 8	K11455	
PGCF2	PGCF2, RNF110; polycomb group RING finger protein 2	K11460	
PGCF4	PGCF4, BMI1; polycomb group RING finger protein 4	K11459	
PHC1	PHC1, EDR1; polyhomeotic-like protein 1	K11456	
RING1	RNF1_2; E3 ubiquitin-protein ligase RNF1/2 [EC:6.3.2.19]	K10695	
SCMH1	SCMH1; polycomb protein SCMH1	K11461	
PRC2-EZH2 complex			
EZH2	EZH2; histone-lysine N-methyltransferase EZH2 [EC:2.1.1.43]	K11430	LC100104
EED	EED; polycomb protein EED	K11462	
SUZ12	SUZ12; polycomb protein SUZ12	K11463	
RBBP4	RBBP4, HAT2, CAF1, MIS16; histone-binding protein RBBP4	K10752	
AEBP2	AEBP2; zinc finger protein AEBP2	K17452	
Other polycomb group proteins			
PCGF3	PCGF3; polycomb group RING finger protein 3	K11488	LC100109
MTF2	MTF2, PCL2; polycomb-like protein 2	K11485	
HMTs (histone methyltransferases)			
HKMTs (histone lysine methyltransferases)			
SETMAR	SETMAR; histone-lysine N-methyltransferase SETMAR [EC:2.1.1.43]	K11433	
PRMTs (protein arginine methyltransferases)			
PRMT5	PRMT5, HSL7; protein arginine N-methyltransferase 5 [EC:2.1.1.125]	K02516	
Other heterochromatin formation proteins			
DNMT1	DNMT1, dcm; DNA (cytosine-5)-methyltransferase 1 [EC:2.1.1.37]	K00558	
Methyltransferases			
DNMT2	TRDMT1, DNMT2; tRNA (cytosine38-C5)-methyltransferase	K15336	

**G. cornutus* CBX6 was identified as the most homologous gene for *Tribolium Castaneum* CBX6 by BLAST.

Table S5. List of primer sequences for RNAi and injected dose conditions.

Gene	Forward primer 5' -3'	Reverse primer 5' -3'	late KD		early KD
			viable pupa	viable adult	
GFP (see References 3)	GFPIF2: TAATACGACTCACTATAGGGC GATGCCACCT	GFPIF5: TAATACGACTCACTATAGGGCGGACTGG GTG	50.6 ng	50.6 ng	50.6 ng
HDAC1	TAATACGACTCACTATAGGGT CCAAGCAATATGGGCAATC	TAATACGACTCACTATAGGGGACGGAGT TGGTCCCGTATC	50.6 pg	5.06 pg	5.06 pg
HDAC3	TAATACGACTCACTATAGGGT TTTTGCCCCCGACTTTACG	TAATACGACTCACTATAGGGGAGGTTTCCA TTTCTTCCTTATCGT	50.6 ng	0.506 ng	0.506 ng
HDAC4	TAATACGACTCACTATAGGGG GAAGGAGGCTACGATCTGC	TAATACGACTCACTATAGGGGGCGAACA ACCTGGGTGATA	5.06 ng	5.06 ng	
HDAC6	TAATACGACTCACTATAGGGC CGATTGTAATGCCGAGAGA	TAATACGACTCACTATAGGGTTGGAAGT TTAAAAGCGTTG	50.6 ng	50.6 ng	
HDAC11	TAATACGACTCACTATAGGGT AGTGTACCGCCCCGAGTAC	TAATACGACTCACTATAGGGCAGTTTTCC GGCCAAAATAG	50.6 ng	50.6 ng	
EZH2	TAATACGACTCACTATAGGGG TGCCCAGAGAACAAACCAT	TAATACGACTCACTATAGGGGAGGATTCGT GTTACCGTTCCG	50.6 ng	50.6 ng	
PCGF3	TAATACGACTCACTATAGGGG TCCCCACAAGAACCACTGT	TAATACGACTCACTATAGGGGAGTCAAAAA TCGGCTGCAAT	50.6 ng	50.6 ng	

The maximum dose for viable pupa represents the highest dose of RNAi that enables pupal development. For HDAC1 and HDAC3, this dose caused lethality during the pupal stage; thus, the dose was further lowered to allow adult eclosion (maximum dose for viable adult). All other RNAi experiments successfully yielded the adult, so further adjustment was not performed.

Table S6. Effects of HDAC1 and HDAC3 late-knockdowns on trait sizes.

Trait	Relative size change	Sample size		Effect (treatment)		Effect (treatment x elytra width)	
	(% of GFP control)	GFP	Treatment	<i>F</i>	<i>P</i>	<i>F</i>	<i>P</i>
HDAC1 knockdown							
mandible length (ML)	-3.00%	20	20	1.733	0.196	4.074	0.051
mandible outline length (MOL)	-9.80%	20	20	20.286	0.000	1.918	0.175
mandible width (MW)	-4.90%	20	20	5.316	0.027	0.007	0.934
gena width (GW)	-1.60%	20	20	1.345	0.254	0.204	0.654
prothorax width (PW)	-1.50%	20	20	5.952	0.020	0.64	0.429
maximum prothorax width (MPW)	-0.30%	20	20	0.001	0.980	0.292	0.592
fore femur length (FFL)	-0.40%	20	19	0.15	0.700	3.485	0.070
fore femur width (FFW)	1.10%	20	20	1.306	0.261	0.821	0.371
mid femur length (MFL)	0.20%	19	20	0.332	0.568	0.621	0.436
mid femur width (MFW)	1.50%	19	20	1.883	0.178	0.001	0.974
hind femur length (HFL)	0.80%	20	20	0.011	0.916	4.072	0.051
hind femur width (HFW)	0.30%	20	19	0.255	0.616	2.587	0.116
genitalia length (GL)	-0.70%	17	20	0.877	0.356	0.089	0.767
wing vein length-1 (WVL-1)	4.40%	20	19	16.14	0.000	0.205	0.654
wing vein length-2 (WVL-2)	3.90%	20	19	11.435	0.002	0.456	0.504
HDAC3 knockdown							
mandible length (ML)	-	20	20	-	-	5.459	0.025
mandible outline length (MOL)	12.80%	20	20	34.394	0.000	2.561	0.118
mandible width (MW)	20.00%	20	20	70.231	0.000	0.205	0.653
gena width (GW)	-0.30%	20	20	0.084	0.773	1.386	0.247
prothorax width (PW)	-	20	20	-	-	7.573	0.009
maximum prothorax width (MPW)	-1.90%	20	20	5.466	0.025	2.346	0.134
fore femur length (FFL)	-1.80%	20	18	2.133	0.153	1.405	0.244
fore femur width (FFW)	-0.80%	20	20	0.44	0.511	2.306	0.138
mid femur length (MFL)	-0.20%	19	20	0.6	0.444	0.69	0.412
mid femur width (MFW)	2.00%	19	20	3.285	0.078	0.966	0.332
hind femur length (HFL)	-0.60%	20	20	0.52	0.475	1.44	0.238
hind femur width (HFW)	2.30%	20	19	2.984	0.093	1.435	0.239
genitalia length (GL)	-0.60%	17	19	0.271	0.606	0.001	0.978
wing vein length-1 (WVL-1)	-2.40%	20	18	5.631	0.023	0.181	0.673
wing vein length-2 (WVL-2)	-3.50%	20	18	10.312	0.003	0.12	0.731

Relative trait sizes were calculated as estimated marginal means (adjusted means) at mean body size with elytra width as a covariate by ANCOVA. Bold letters indicate significant size changes when compared with the GFP RNAi control.

Table S7. Effects of HDAC1 and HDAC3 early-knockdowns on trait sizes.

Trait	Relative size change (% of GFP control)	Sample size		Effect (treatment)		Effect (treatment x elytra width)	
		GFP	Treatment	<i>F</i>	<i>P</i>	<i>F</i>	<i>P</i>
HDAC1 early-knockdown							
mandible length (ML)	-9.50%	20	20	12.626	0.001	0.265	0.610
mandible outline length (MOL)	-13.49%	20	20	27.950	0.000	0.015	0.902
mandible width (MW)	-14.22%	20	20	35.832	0.000	0.447	0.508
gena width (GW)	0.49%	20	20	0.858	0.360	0.012	0.912
prothorax width (PW)	-0.70%	20	20	1.120	0.297	0.076	0.784
maximum prothorax width (MPW)	-0.40%	20	20	0.743	0.394	0.139	0.711
fore femur length (FFL)	0.32%	20	20	0.131	0.719	2.738	0.107
fore femur width (FFW)	-0.32%	20	20	0.250	0.620	2.351	0.134
mid femur length (MFL)	-0.59%	20	20	1.225	0.276	0.006	0.941
mid femur width (MFW)	-1.10%	20	20	1.804	0.187	0.020	0.888
hind femur length (HFL)	-0.95%	20	20	2.845	0.100	0.221	0.641
hind femur width (HFW)	0.79%	20	20	0.812	0.373	0.184	0.671
genitalia length (GL)	0.27%	20	20	0.046	0.832	0.000	0.995
wing vein length-1 (WVL-1)	1.61%	20	20	9.223	0.004	0.159	0.692
wing vein length-2 (WVL-2)	1.62%	20	20	9.189	0.004	0.484	0.491
HDAC3 early-knockdown							
mandible length (ML)	2.44%	20	20	1.453	0.236	0.079	0.781
mandible outline length (MOL)	7.48%	20	20	31.931	0.000	0.229	0.635
mandible width (MW)	12.46%	20	20	31.262	0.000	0.017	0.898
gena width (GW)	-0.17%	20	20	0.135	0.716	0.318	0.576
prothorax width (PW)	-0.69%	20	20	1.273	0.267	0.018	0.895
maximum prothorax width (MPW)	-0.25%	20	20	0.286	0.596	0.019	0.892
fore femur length (FFL)	0.28%	20	20	0.169	0.684	0.016	0.900
fore femur width (FFW)	1.19%	20	20	2.602	0.115	0.028	0.868
mid femur length (MFL)	0.92%	20	20	1.703	0.200	0.307	0.583
mid femur width (MFW)	0.48%	19	20	0.112	0.740	0.175	0.679
hind femur length (HFL)	-0.67%	20	20	1.402	0.244	2.819	0.102
hind femur width (HFW)	0.78%	20	20	0.275	0.603	1.458	0.235
genitalia length (GL)	-0.56%	20	20	0.256	0.616	0.028	0.868
wing vein length-1 (WVL-1)	0.47%	20	20	0.576	0.453	0.224	0.639
wing vein length-2 (WVL-2)	0.39%	20	20	0.426	0.518	1.562	0.219

Relative trait sizes were calculated as estimated marginal means (adjusted means) at mean body size with elytra width as a covariate by ANCOVA. Bold letters indicate significant size changes when compared with the GFP RNAi control.

Table S8. Factor loadings for principal component analysis.

Trait	PC1 (71.0%)	PC2 (11.1%)	PC3 (9.8%)	PC4 (8.5%)	PC5 (7.2%)
mandible length (ML)	0.859	0.321	-0.105	0.208	0.28
mandible outline length (MOL)	0.724	0.617	0.096	0.293	0.131
mandible width (MW)	0.622	0.695	0.1	0.263	0.208
gena width (GW)	0.967	0.061	-0.245	0.086	-0.336
prothorax width (PW)	0.912	-0.101	-0.278	0.291	-0.509
maximum prothorax width (MPW)	0.955	-0.109	-0.346	0.056	-0.231
fore femur length (FFL)	0.946	-0.077	0.136	0.15	0.054
fore femur width (FFW)	0.95	-0.085	-0.128	-0.081	0.206
mid femur length (MFL)	0.888	-0.135	-0.021	-0.18	0.057
mid femur width (MFW)	0.874	-0.036	-0.326	-0.611	0.042
hind femur length (HFL)	0.723	-0.025	0.689	-0.236	-0.159
hind femur width (HFW)	0.792	0.119	0.521	-0.488	-0.174
genitalia length (GL)	0.758	0.077	0.537	0.501	-0.091
wing vein length-1 (WVL-1)	0.726	-0.603	-0.05	-0.034	0.499
wing vein length-2 (WVL-2)	0.729	-0.603	0.001	0.057	0.406

Note that detrended data (residuals of linear regression on body size (elytra width) were subjected to PCA. Strong loading factors in given PCs (correlation coefficient between the trait and the PC at $P < 0.001$ level) are highlighted in bold letters.

Table S9. Effects of EZH2 and PCGF3 knockdowns on mandible sizes.

Trait	Relative size change	Sample size		Effect (treatment)		Effect (treatment x elytra width)	
	(% of GFP control)	GFP	Treatment	<i>F</i>	<i>P</i>	<i>F</i>	<i>P</i>
EZH2 knockdown							
mandible length (ML)	-	20	20	-	-	18.633	0.000
mandible outline length (MOL)	-	20	20	-	-	4.337	0.044
mandible width (MW)	-29.40%	20	20	112.134	0.000	2.394	0.131
PCGF3 knockdown							
mandible length (ML)	-	20	20	-	-	19.167	0.000
mandible outline length (MOL)	-	20	20	-	-	9.667	0.004
mandible width (MW)	-25.80%	20	20	98.233	0.000	1.926	0.174

Relative trait means were calculated as estimated marginal means (adjusted means) at mean body size with elytra width as a covariate by ANCOVA. Bold letters indicate significant size changes when compared with the GFP RNAi control.

Table S10. List of primer sequences for quantitative RT-PCR.

Gene	Foreword primer 5' - 3'	Reverse primer 5' - 3'
HDAC1	TGCAAACACGCTGTTAGTGC	CAAAACCTTCGCACTAGACTTG
HDAC3	ACAACACCTCGCTTCTCGTT	TGAAGCTCCTTCCACACGTA
HDAC4	TTAAAACAACGCGTGATGGA	GCTCTTGAGGAGGTGATTCG
HDAC6	GGATAAGAAGAAGGGCAGAGG	CAACGACAATGGTTTCATCG
HDAC11	ACGGGAAATGAACACTTTGG	CGCAAACACAAACAACTGC
EZH2	CGCTGATGCAGTACCAAGAA	AGGAAATTGCGTGGAATTG
PCGF3	GGTCCCTGAATTGCAGAAAG	GTACGTCGGCTGATGGTTTT
ACTIN	CCCATACCGACCATGAC	TCCGGTATGTGCAAAGCC